

## X-ray diffraction investigation of a spin crossover hysteresis loop

This article has been downloaded from IOPscience. Please scroll down to see the full text article.

2007 J. Phys.: Condens. Matter 19 326211

(<http://iopscience.iop.org/0953-8984/19/32/326211>)

View [the table of contents for this issue](#), or go to the [journal homepage](#) for more

Download details:

IP Address: 129.252.86.83

The article was downloaded on 28/05/2010 at 19:58

Please note that [terms and conditions apply](#).

## X-ray diffraction investigation of a spin crossover hysteresis loop

P Guionneau<sup>1</sup>, F Le Gac<sup>1</sup>, S Lakhoufi<sup>1</sup>, A Kaiba<sup>1</sup>, D Chasseau<sup>1</sup>,  
J-F Létard<sup>1</sup>, P Négrier<sup>2</sup>, D Mondieig<sup>2</sup>, J A K Howard<sup>3</sup> and J-M Léger<sup>4</sup>

<sup>1</sup> ICMCB, CNRS, Université Bordeaux I, 87 avenue du Dr A Schweitzer, 33608 Pessac Cedex, France

<sup>2</sup> Centre de Physique Moléculaire Optique et Hertzienne, UMR Université Bordeaux I CNRS 5798, 33405 Talence Cedex, France

<sup>3</sup> Chemical Crystallography Group, Chemistry Department, Durham University, South Road, Durham DH1 3LE, UK

<sup>4</sup> Laboratoire de Pharmacochimie, Université Victor Segalen Bordeaux II, 146 rue Léo Saignat, 33076 Bordeaux, France

E-mail: [guio@icmcb-bordeaux.cnrs.fr](mailto:guio@icmcb-bordeaux.cnrs.fr)

Received 10 January 2007, in final form 20 June 2007

Published 16 July 2007

Online at [stacks.iop.org/JPhysCM/19/326211](http://stacks.iop.org/JPhysCM/19/326211)

### Abstract

The nature and the mechanism of the magnetic hysteresis for the thermal spin crossover exhibited by an iron (II) compound is investigated by means of variable-temperature powder and single-crystal x-ray diffraction. The unit cell temperature dependence clearly evidences the amplitude of the strong structural rearrangement that accompanies the spin crossover—*corresponding to a variation of 8.6% for one of the unit cell parameters*—as well as the structural hysteresis width. In this regard, the present x-ray study reveals significant differences in the spin crossover features according to the nature of the sample—*powder or single crystal*—that should be taken into account in the analysis of physical properties. Concerning the interplay between structural and magnetic transitions, quenching effects show that the structural transition and the spin crossover are indissociable. Furthermore, investigations of the mechanism itself of the thermal spin crossover confirm the presence of spin-like domains in the conversion region, either in the cooling or in the warming loops. The non-dependence with temperature of these domains inside the hysteresis loop demonstrates the stability of the microscopic and macroscopic structures in the corresponding thermodynamic conditions. This result is of interest in the context of the potential use of hysteresis loops to obtain high-temperature photo-conversion.

(Some figures in this article are in colour only in the electronic version)

## 1. Introduction

The solid-state reversible modification of the electronic configuration in a transitional-metal ion from a high-spin (HS) state to a low-spin (LS) state, namely the spin crossover, is increasingly studied either for fundamental interests or potential applications [1]. It is well known that the spin crossover driven by a variation of temperature and pressure or by an electromagnetic radiation exhibits a wide range of magnetic, optical and structural features that are very promising for the design of electronic molecular devices. However, some points still need to be elucidated or at least to be explored more deeply in order to be able to design efficient spin crossover devices. This is for instance the case of the mechanism of spin crossover propagation through a material, which may affect the switching time.

In regard to the mechanism of the spin crossover phenomenon, one of the crucial points still to be elucidated concerns the distribution of the entities that adopt the same spin state through the macroscopic sample when the conversion is not complete, as for example at the temperature  $T_{1/2}$ , where half of the entities are in the HS state and half in the LS state. Three situations could be envisaged *a priori*: (1) a random repartition corresponding to a homogeneous distribution at the sample scale, (2) a spin-like domain repartition where all the entities within a same domain adopt the same spin state, or (3) the occurrence of an intermediate structural phase where HS and LS entities are structurally ordered. These situations can be easily distinguished experimentally through variable-temperature x-ray diffraction: situation (1) gives Bragg peaks reflecting an average of the microscopic distribution, with the position of the peaks continuously changing with temperature; situation (2) gives a split of each Bragg peak into an HS and an LS component such that the positions of these peaks barely change with temperature, while the intensities increase or decrease proportionally to the macroscopic spin conversion level; and situation (3) corresponds to a significant change in the reciprocal space as at least two entities must be structurally independent.

Despite early preliminary attempts [2], it is only very recently that accurate x-ray diffraction experiments have been conducted to investigate the mechanism of transition. Spin domains, (2), have been observed either for the thermal or the photo-induced spin crossover in a few materials [3–6] and examples of a continuous process, (1), [7] and of an intermediate structural phase, (3), [8] have been reported. More intricate phenomena like incommensurate modulating have also been observed [9].

Moreover, one recurrent question about the mechanism of the spin crossover phenomenon concerns the links between structural and spin transitions. Does the former drive the latter or vice versa?

Within this context, we investigated the mechanism along and inside a hysteresis loop as well as the synergy between the spin transition and the structural transition in the mononuclear iron (II) complex showing one of the largest magnetic hysteresis loops, namely  $[\text{Fe}(\text{PM-PEA})_2(\text{NCS})_2]$ , (PM-PEA = *N*-2'-pyridylmethylene-4-phenylethynyl and NCS = thiocyanate) [10].

## 2. Experimental details

### 2.1. X-ray powder diffractograms in the range 100–300 K

In order to cover the hysteresis loop, x-ray diffractograms were recorded every 10 K when cooling from 280 to 120 K and then when warming up from 120 to 280 K with additional recordings around  $T_{1/2}$ , which corresponds to the temperature at which half of the complexes are in the LS state. Moreover, in order to investigate inside the hysteresis loop, diffractograms were registered every 5 K starting from 188 K, which corresponds to  $T_{1/2}$  in the cooling

mode, namely  $T_{1/2\downarrow}$ , by warming directly to 238 K, which corresponds to  $T_{1/2}$  in the warming mode, namely  $T_{1/2\uparrow}$ . X-ray high-resolution diffraction patterns were recorded by means of a horizontally mounted INEL cylindrical position-sensitive detector (CPS 120) by gas ionization (argon + C<sub>2</sub>H<sub>6</sub>) using Debye–Scherrer geometry (angular step about  $0.029^\circ - 2\theta$ ) [11]. Monochromatic Cu  $K\alpha_1$  radiation was selected as the incident beam. Low-temperature measurements were achieved with an Oxford Cryosystems N<sub>2</sub> cryostream, which provided isothermal experiments at different temperatures. The generator power was set to 40 kV and 25 mA. Samples were introduced in 0.5 mm diameter Lindemann glass capillaries, rotating around their axes during the experiment in order to minimize preferential orientations of the crystallites. The acquisition time was set to an hour in order to obtain reflections with exploitable intensities. External calibration using Na<sub>2</sub>Ca<sub>3</sub>Al<sub>2</sub>F<sub>14</sub> [12] cubic phase combined with a low-angle calibration using silver behenate [13] was performed by means of cubic spline fittings.

## 2.2. Accurate unit cell from single-crystal experiments in the range 140–280 K

Most of the single crystals explode at the spin transition due to the strong structural modifications. Very small prismatic single crystals of approximate dimensions of 10  $\mu\text{m}$  were consequently used because they are less affected by such deterioration. Moreover, the crystals were coated in an oil in the expectation of limiting the damages induced by the transition. In order to get enough diffraction peaks, the temperature dependence of the unit cell was investigated using a Rigaku Rapid R-axis diffractometer using a MM007 microfocus rotating-anode generator with Cu radiation.

## 2.3. Quenching single-crystal experiments

Single crystals were flash cooled to 30 K and investigated using an Oxford Cryosystems Helix open-flow He gas cryostat combined with a Bruker SMART-CCD area-detector diffractometer using Mo  $K\alpha$  radiation. First a full data collection was performed at 30 K. The diffraction frames were integrated using the SAINT package [14]. The structural determination by direct methods and the refinement of the atomic parameters based on full-matrix least squares on  $F^2$  were performed using the SHELX-97 [15] programs within the WINGX package [16]. Crystal data: 30 K,  $a = 15.681(1)$  Å,  $b = 14.192(1)$  Å,  $c = 16.634(2)$  Å,  $\beta = 93.18(1)^\circ$ ,  $V = 3696(1)$  Å<sup>3</sup>, monoclinic  $P2_1/c$ , 20925 collected reflections for 7916 independent ( $R_{\text{int}} = 0.04$ ),  $R = 0.047$ ,  $wR2 = 0.109$ . Full experimental and crystal data can be obtained from the supplementary crystallographic data for this paper, number CCDC-632777.

After data collection at 30 K, unit cell parameters were determined by warming the sample. The experiments were reproduced. All investigated samples show no modification of the unit cell from 30 to 60 K. The diffraction pattern changes at around 65(5) K and all the samples are strongly damaged, as usually observed at the spin crossover for this compound, indicating the HS to LS relaxation at this temperature.

## 3. Results and discussions

### 3.1. Unit cell along the hysteresis loop

The iron (II) mononuclear complex denoted [Fe(PM-PeA)<sub>2</sub>(NCS)<sub>2</sub>] is known to exhibit a thermally induced spin crossover with a large hysteresis. Magnetic measurements give a temperature of transition of  $T_{1/2\downarrow} = 188$  K when cooling and  $T_{1/2\uparrow} = 238$  K when warming, showing a hysteresis of 40 K [10]. Previous x-ray structural investigation indicated a

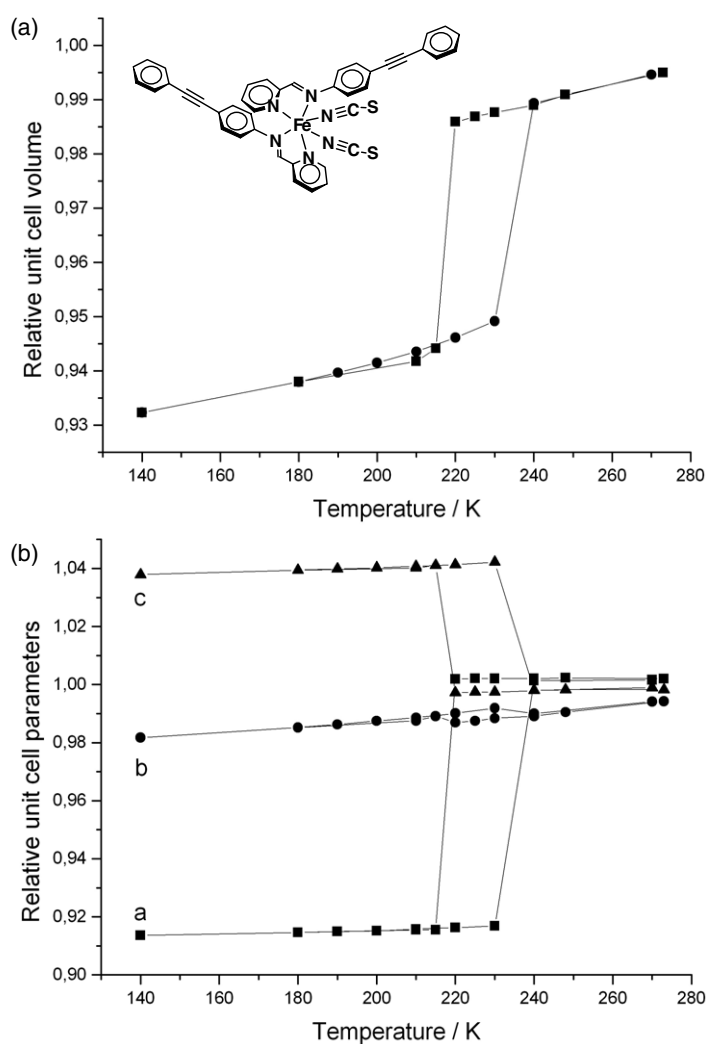


**Figure 1.** Relative unit cell temperature dependence along the hysteresis loop: (a) unit cell volume (b) unit cell parameters *a* (square), *b* (circle) and *c* (triangle) determined by mean of single-crystal x-ray diffraction. References are the 280 K unit cell parameters  $a = 15.669(1) \text{ \AA}$ ,  $b = 14.535(1) \text{ \AA}$ ,  $c = 16.865(2) \text{ \AA}$ ,  $\beta = 93.18(1)^\circ$ ,  $V = 3834(1) \text{ \AA}^3$ . The molecular scheme of the complex is inserted.

strong rearrangement at the spin crossover from a monoclinic  $P2_1/c$  unit cell in the HS state to an orthorhombic  $Pccn$  unit cell in the LS state [17]. Up to now the unit cell temperature dependence along the hysteresis loop could not be determined due to the deterioration of the samples at the structural transition. This has been achieved here by single-crystal x-ray diffraction (figure 1). The determination of the unit cell parameters and volume variations from 280 to 140 K in the warming and cooling modes confirms the structural transition and evidences an hysteresis width of 19 K.

First, the temperatures of the transition deduced from the structural data do not correspond to those obtained by magnetic measurements, especially in the cooling mode:  $T_{1/2\downarrow} = 215 \text{ K}$  when cooling and  $T_{1/2\uparrow} = 234 \text{ K}$ . The small difference for the latter

(4 K) can easily be explained by taking into account experimental errors, but the former shows a significant difference of 17 K not explained at present. Both magnetic and x-ray measurements are reproducible. One can note, however, that the magnetic measurements were performed on a powder sample or on a large number of single crystals, while the x-ray experiments were performed on one single crystal only. No differences have been observed between the experimental powder diffractogram and the diffractogram simulated from the single-crystal structure atomic parameters. This indicates that the crystallographic phases are identical. However, it is well known that spin crossover characteristics are very sensitive to crystal defects, especially solvent inclusion. The family of complexes to which  $[\text{Fe}(\text{PM-PeA})_2(\text{NCS})_2]$  belongs is indeed known to be potentially affected by solvent inclusion [17]. If these defects affect the samples randomly then magnetic measurements based on the use of a large amount of crystallite are more likely affected. The presence of defects is thus probably at the origin of the above differences. The single-crystal x-ray diffraction experiment was repeated a few times and gave the same results. This is coherent with the fact that all single crystals found in the crystallization tube and thus used for the present experiment are free of solvent inclusions. It would of course be interesting to get single crystals of this compound containing solvent inclusions, as has been obtained for complexes of the same series [17], in order to definitively screen the effect of solvent inclusion on the hysteresis width. Efforts are currently being made to do this. In any case, this means that one has to be very careful when giving a spin crossover temperature and one should always be precise about the nature of the sample—powder or single crystal—especially when the kind of complex is known to be potentially affected by defects. The powder measurements reflect the distribution of temperatures exhibited by grains affected at different levels by defects, while the single-crystal measurements reflect the temperature for the single crystal in question, and, as it is shown here, significant differences can be observed.

The amplitude of the volume variation of the sample at the macroscopic level is an interesting feature, as it could be used in a large number of potential applications, such as molecular motors, for instance [18]. The macroscopic modification of the crystal follows the modification of the unit cell. The unit cell temperature dependence shows that the spin transition corresponds to a reversible modification of the unit cell volume of 4.2%, which is by far the largest change observed for a mononuclear complex (figure 1(a)). However, the anisotropy of the unit cell modification (figure 1(b)) appears to be one of the main characteristics of the structural modification of this compound at the spin transition. Indeed, the  $b$  parameter is not affected by the transition ( $-0.2\%$ ) while the  $c$  parameter increases ( $+4.4\%$ ) and the  $a$  parameter strongly decreases ( $-8.6\%$ ) from HS to LS. The amplitudes of the modification are strictly the same from LS to HS but obviously in the opposite sense. These unit cell modifications correspond by definition to the macroscopic sample modifications at the spin crossover that consequently are strongly anisotropic. The anisotropy of the unit cell parameters modifications due to the spin transition appears to be a general feature [19], but it is unusually pronounced in the present case. As a general matter of fact, the anisotropy of the *contraction–dilatation process* at the spin crossover should therefore be taken into account in any attempt to use the sample volume variation in a potential application.

### 3.2. Simultaneity of structural and spin transitions

Concerning the mechanism of spin crossover, knowing which of the structural transition and the spin crossover drives the other one often corresponds to a *chicken and egg* problem. In the present case, the occurrence of a large structural reorganization corresponding to a change of unit cell symmetry, from monoclinic  $P2_1/c$  to orthorhombic  $Pccn$ , represents the opportunity

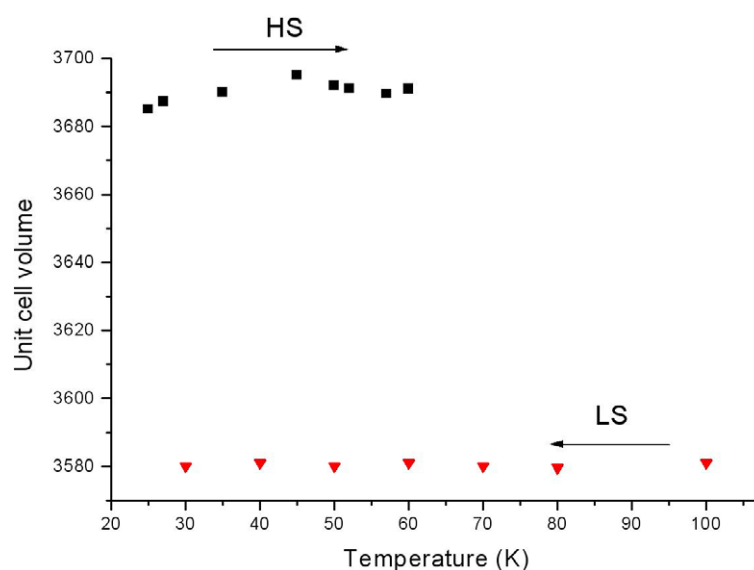


**Figure 2.** Temperature dependence of the unit cell volume after a quench at 30 K (square) or a slow cooling (triangle). Single crystals are seriously damaged during the HS to LS relaxation.

to study the simultaneity of the structural and spin transitions. We tried to differentiate these phenomena by investigating the quenching effect. A single crystal was rapidly cooled from 293 to 30 K and the crystal structure determined. The monoclinic–orthorhombic transition is quenched. The 30 K unit cell is very close to the high-temperature HS one. The crystal packing is identical to the already known HS crystal structure at room temperature [10]. The iron (II) coordination sphere geometry also clearly indicates that the complexes are in the HS state, even though a small LS residue cannot be excluded, as shown by the metal–ligand bond lengths ( $\langle \text{Fe–N} \rangle = 2.107(1) \text{ \AA}$ ) and the distortion parameters ( $\Sigma = 73.7(1)^\circ$ ) in agreement with the HS values for this kind of complex [19]. This result evidences in the present case the synergy between the structural transition and the spin conversion, showing that they cannot be dissociated. This is enhanced by the unit cell parameter temperature dependence by warming after a quench at 30 K (figure 2). Unsurprisingly, the unit cell volume relaxes towards the unit cell volume expected after a slow cooling. It has been indeed previously demonstrated, from magnetic and structural measurements, that quenched HS states relax towards the LS state after warming [20]. The deterioration of the single crystals in this process is clearly in line with the structural transition, known to be destructive for the single crystal in this sample. Thus, the spin conversion and structural transition cannot be differentiated in this sample and they probably must not be seen as separated phenomena.

This result also shows that for this compound the temperature beyond which a photo-conversion is efficient, namely  $T(\text{LIESST})$  [21], is the same that the temperature corresponding to the HS to LS conversion after quenching, namely  $T(\text{TIESST})$ . For the studied complex, the former has been determined at 65(2) K by magnetic measurements on single crystals [22] and the present study shows that the latter is around 65(5) K.

### 3.3. Spin-like domain temperature dependence

The single-crystal investigation unambiguously characterizes a spin-like domain distribution, referring to process (2) described above, as shown by the reversible splitting of the Bragg

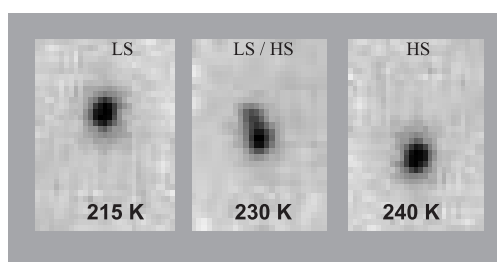


**Figure 3.** Temperature dependence of a diffraction spot in a single-crystal x-ray experiment showing the splitting of the Bragg peak due to spin-like domains in the conversion temperature region.

peaks in the spin crossover zone (figure 3). However, the alteration of the single crystals around this temperature encouraged us to investigate the temperature dependence of the spin domains in powder samples in order to obtain reliable quantitative data. Analysis of the powder diffractograms clearly confirms the spin-like domain mechanism of the transition for this compound (figure 4). This is especially clear for the more intense Bragg peak (110) on which we can focus. As expected for spin domains, in the cooling mode the LS component appears around 205 K, when the intensity of the HS component starts to decrease, and it is unique at around 165 K, when the HS component is no longer observable. Then, in the warming mode, the HS component reappears at around 215 K to be unique at around 235 K. The hysteresis loop is consequently perfectly described by the spin domain formation process.

The (110) Bragg peak intensity temperature dependence (figure 5) first shows that the spin conversion region corresponds to a coexistence of the HS and LS spin domains on a large temperature range of about 40 K in the cooling mode and 20 K in the warming mode. Consequently, the transition is not as abrupt as expected, especially in the cooling mode. Note that these results are strictly reproducible either in subsequent complete thermal cycles or on other samples.

The temperatures for which the intensities of the HS and LS (110) Bragg peaks are identical give the  $T_{1/2}$  values in the corresponding mode,  $T_{1/2\downarrow} = 190$  K and  $T_{1/2\uparrow} = 232$  K. The hysteresis width appears thus to be of around 40 K. These values are in line with those deduced from the magnetic measurements that were also performed on powder or/and on a large number of single crystals, but the hysteresis width is around half that obtained from the x-ray investigation on the single crystal reported above, i.e. 20 K. As already noticed above, the latter can certainly be considered as the structural hysteresis width corresponding to a crystal packing free of solvent inclusion. Indeed, measurements performed on a powder or equivalent sample probably mirror some additional inhomogeneity within the grains. This is for example reflected by the (110) intensity temperature dependence curves that present an asymmetric shape near  $T_{1/2}$ , the low-temperature modifications being smoother than the high-temperature ones. The nature of this inhomogeneity is to be determined, but it may find its origin in crystal defects.

Elsewhere, it has been recently demonstrated from spectroscopic measurements on other iron spin crossover complexes that it is possible in certain conditions to induce a photo-conversion within the hysteresis loop using a pulsed laser beam at room temperature [23]. These promising results question, however, the stability of the structure of the sample at the microscopic and macroscopic levels within the hysteresis loop. This stability appears crucial for the non-fatiguability and the reproducibility of the conversion within the hysteresis loop. The iron (II) compounds studied, for which no single crystals were available, were however known to be easily photo-switchable. In the case of  $[\text{Fe}(\text{PM-PeA})_2(\text{NCS})_2]$  the core of the



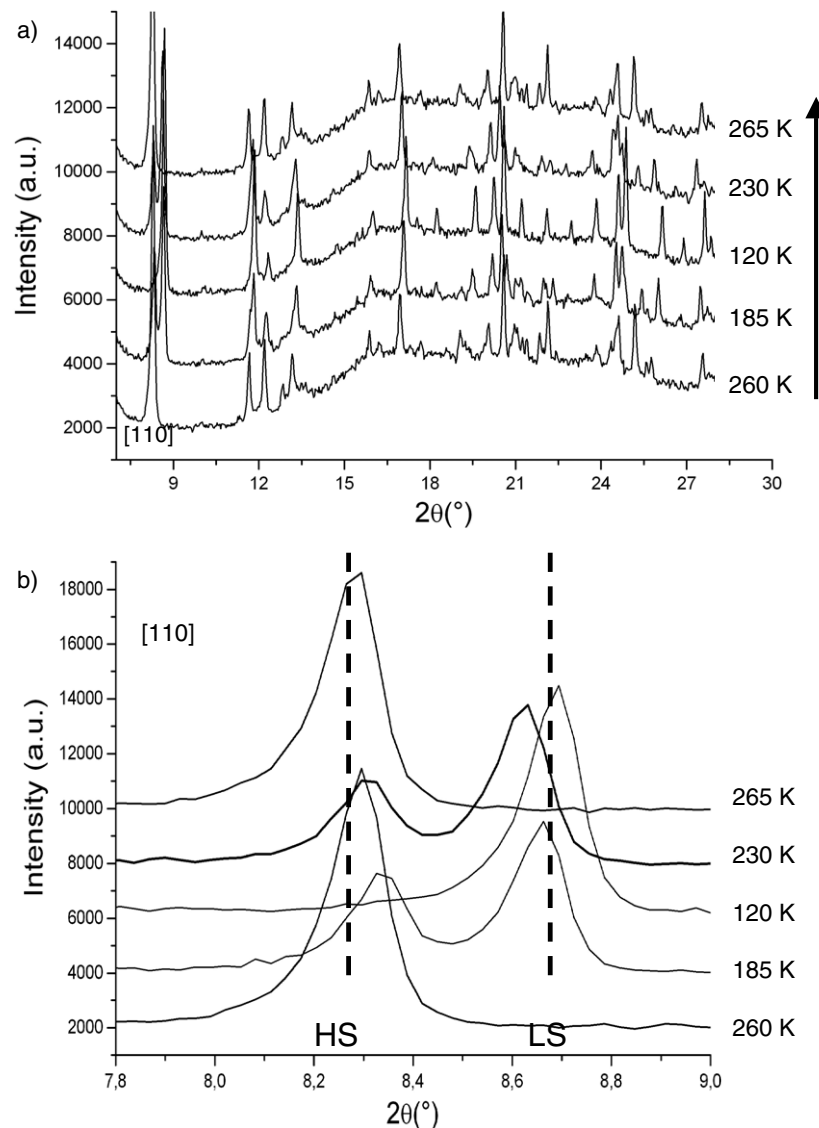


**Figure 4.** (a) Selected x-ray powder diffractograms along the hysteresis loop and (b) enlargement of the (110) Bragg peak showing the reversible splitting of the peaks. Data are recorded by cooling from 260 to 120 K then by warming from 120 to 265 K.

loop cannot be accessed by irradiation effects but it is possible to access it by temperature effects instead. Even though no spin crossover is expected by thermal effects in the hysteresis loop, an x-ray investigation can give preliminary information on the thermal stability of the sample in this loop. The sample was thus first cooled down to  $T_{1/2\downarrow}$  and the Bragg peaks shapes were then registered every 5 K from  $T_{1/2\downarrow}$  to  $T_{1/2\uparrow}$  from powder diffractograms. This allows one to follow the temperature dependence of the HS to LS ratio of the spin-like domains (figure 6). First, the shape of the corresponding HS and LS Bragg peaks remains unchanged in all the hysteresis loop, testifying no modifications of these domains. This result also proves

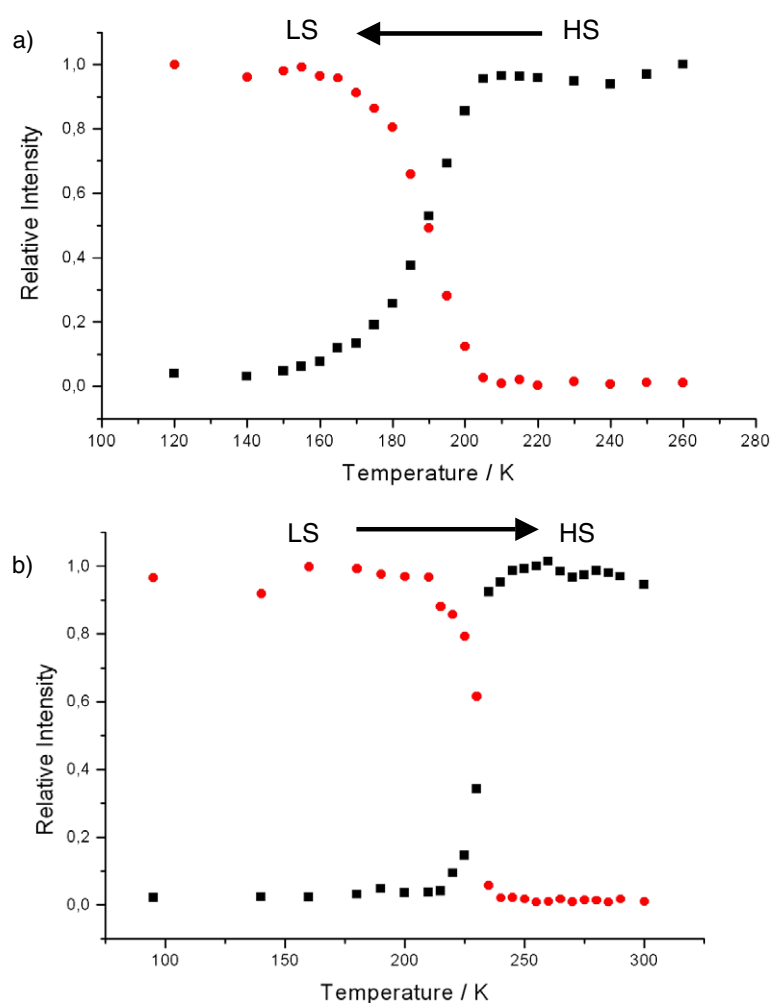


**Figure 5.** Detailed temperature dependence of the intensity of the (110) Bragg peaks corresponding to the HS (square) and the LS (circle) domains (a) in the cooling mode and (b) in the warming mode.

that the samples are not damaged by such warming at any scale. The intensities of the Bragg peaks are not modified during the warming up to  $T_{1/2\uparrow}$ . This indicates that ratio of the HS and LS domains (0.5) is not affected by such warming. Consequently, this spin-like domain temperature dependence from  $T_{1/2\downarrow}$  to  $T_{1/2\uparrow}$  demonstrates the thermal stability of the sample at the microscopic and the macroscopic levels inside the magnetic hysteresis loop.

#### 4. Conclusions

The investigation of the  $[\text{Fe}(\text{PM-PeA})_2(\text{NCS})_2]$  complex first confirms that one has to be very careful when comparing spin crossover features from experiments performed using powder and single-crystal samples. In particular, temperatures of transition can be very sensitive to the nature of the sample, probably because of the possible presence of crystal defects. Then, it has been shown that the very large and anisotropic unit cell modifications and the spin crossover phenomenon are probably indissociable in the present case. Elsewhere, x-ray powder

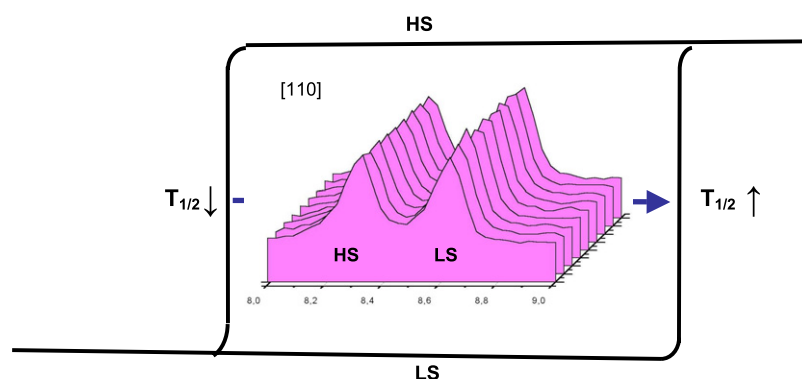


**Figure 6.** Temperature dependence of the intensity and of the shape of the (110) Bragg peaks corresponding to the HS and the LS domains inside the hysteresis loop. Powder diffraction scans are taken every 5 K from 190 to 230 K.

diffraction has been evidenced as a powerful tool to visualize and investigate the mechanism of the transition, screening here a spin-like domain process. Investigation of the hysteresis loop has revealed that it is possible to navigate inside the loop without damaging the sample and without modifying the spin-like domain shapes and ratios. One of the new routes to get photo-induced high-temperature spin crossover devices aims at inducing the conversion inside the hysteresis loop [23, 24]. In this regard the present results stating the microscopic and macroscopic thermal stability of the sample inside the loop represent an encouraging feature. Obviously, in order to go further on that point, x-ray investigations of the photo-conversion inside a hysteresis loop should now be attempted on a well-selected compound, for example, by means of time-resolved x-ray diffraction.

## References

- [1] Gütllich P and Goodwin H A (ed) 2004 *Spin Crossover in Transition Metal Compounds (Topics in Current Chemistry vol I, II and III)* (Berlin: Springer)
- [2] Irlor W, Ritter G, König E, Goodwin H A and Nelson SM 1979 *Solid State Commun.* **29** 39
- [3] Pillet S, Hubsch J and Lecomte C 2004 *Eur. J. Phys. B* **38** 541
- [4] Huby N, Guérin L, Collet E, Toupet L, Ameline J C, Cailleau H, Roisnel T, Tagayaki T and Tanaka K 2004 *Phys. Rev. B* **69** 020101(R)
- [5] Ichiyonagi K, Hebert J, Toupet L, Cailleau H, Guionneau P, Létard J-F and Collet E 2006 *Phys. Rev. B* **73** 060408(R)
- [6] Legrand V, Carbonera C, Pillet S, Souhassou M, Létard J F, Guionneau P and Lecomte C 2005 *J. Phys.: Conf. Ser.* **21** 73
- [7] Goujon A, Gillon B, Debede A, Cousson A, Gukasov A, Jęftic J, McIntyre G J and Varret F 2006 *Phys. Rev. B* **73** 104413
- [8] Chernyshov D, Hostettler M, Tönroos K W and Bürgi H B 2003 *Angew. Chem. Int. Edn* **42** 3825
- [9] Pillet S, Lecomte C, Sheu C F, Lin Y C, Hsu I J and Wang Y 2005 *J. Phys.: Conf. Ser.* **21** 221
- [10] Létard J-F, Guionneau P, Codjovi E, Olivier L, Bravic G, Chasseau D and Kahn O 1997 *J. Am. Chem. Soc.* **119** 10861
- [11] Ballou J, Comparat V and Pouxe J 1983 *Nucl. Instrum. Methods* **217** 213
- [12] Evain M, Deniard P, Jouanneaux A and Brec R 1993 *J. Appl. Crystallogr.* **26** 563
- [13] Huang T C, Toraya H, Blanton T N and Wu Y 1993 *J. Appl. Crystallogr.* **26** 180
- [14] 1998 SAINT version 5.0 Bruker Analytical X-ray Instruments, Madison, U.S.A
- [15] Sheldrick G M 1998 *Programs for Crystal Structure Analysis (Release 97-2)* Institut für Anorganische Chemie der Universität, Tammanstrasse 4, D-3400 Göttingen, Germany
- [16] Farrugia L J 1999 *J. Appl. Crystallogr.* **32** 837

- [17] Guionneau P, Létard J-F, Yuffit D S, Chasseau D, Howard J A K, Goeta A E and Kahn O 1999 *J. Mater. Chem.* **4** 985
- [18] Létard J-F, Guionneau P and Goux-Capes L 2004 *Topics Curr. Chem.* **235** 221
- [19] Guionneau P, Marchivie M, Bravic G, Létard J-F and Chasseau D 2004 *Topics Curr. Chem.* **234** 97
- [20] Marchivie M, Guionneau P, Létard J-F, Chasseau D and Howard J A K 2004 *J. Phys. Chem. Solids* **65** 17
- [21] Létard J-F, Guionneau P, Nguyen O, Costa J S, Marcen S, Chastanet G, Marchivie M and Goux Capes L 2005 *Chem. Eur. J.* **11** 4582
- [22] Rosa P 2007 private communication
- [23] Bonhommeau S, Molnar G, Galet A, Zwick A, Real J A, McGarvey J J and Bousseksou A 2005 *Angew. Chem. Int. Edn* **44** 4069
- [24] Freysz E, Montant S, Létard S and Létard J-F 2004 *Chem. Phys. Lett.* **394** 318